Table 1 Suppl. The interaction evidence of predicted functional protein-protein association networks inferred from the 10-leaf and flowering stages showed in Fig. 5.

Parameters	Values
Number of nodes	12
Number of edges	14
Average node degree	2.33
Average local clustering coefficient	0.597
Expected number of edges	4
PPI enrichment *P*-value	3.07 E-05

Table 2 Suppl. Functional enrichments of networks inferred from the 10-leaf and the flowering stages showed in the Fig. 5.

Groups	Pathway ID	Pathway description	Count in gene set	False discovery rate
Biological processes	GO:0046686	response to cadmium ion	6	2.79E-06
	GO:0010035	response to inorganic substance	7	5.79E-06
	GO:0006732	coenzyme metabolic process	4	0.00247
	GO:0006091	generation of precursor metabolites and energy	4	0.0031
	GO:0009628	response to abiotic stimulus	6	0.0058
	GO:0072524	pyridine-containing compound metabolic process	3	0.0058
	GO:0006950	response to stress	7	0.00916
	GO:0009266	response to temperature stimulus	4	0.0109
	GO:0046128	purine ribonucleoside metabolic process	3	0.019
	GO:0050896	response to stimulus	8	0.0238
	GO:1901564	nitrogen compound metabolic process	5	0.0298
	GO:0044281	small molecule metabolic process	5	0.0409
	GO:0006096	glycolytic process	2	0.0412
	GO:0009409	response to cold	3	0.0412
	GO:0006081	cellular aldehyde metabolic process	2	0.0445
	GO:0044237	cellular metabolic process	9	0.0485
Cellular components	GO:0009570	chloroplast stroma	6	2.32E-05
	GO:0009507	chloroplast	8	3.07E-05
	GO:0005737	cytoplasm	11	6.15E-05
	GO:0009579	thylakoid	5	6.15E-05
	GO:0048046	apoplast	5	6.15E-05
	GO:0005622	intracellular	11	0.00151
	GO:0044444	cytoplasmic part	9	0.0025
	GO:0005739	mitochondrion	5	0.00254
	GO:0009941	chloroplast envelope	4	0.00259
	GO:0005623	cell	11	0.00382
	GO:0005829	cytosol	5	0.00629
	GO:0044446	intracellular organelle part	7	0.00973
	GO:0044436	thylakoid part	3	0.0113
	GO:0031977	thylakoid lumen	2	0.0116
	GO:0005840	ribosome	3	0.013
	GO:0005759	mitochondrial matrix	2	0.0134
	GO:0009534	chloroplast thylakoid	3	0.0134
	GO:0043231	intracellular membrane-bounded organelle	9	0.0166
	GO:0005618	cell wall	3	0.0294

Table 3 Suppl. Protein-protein interactions in tabular form inferred from the 10-leaf and the flowering stages showed in the Fig. 5.

Node1	Node2	Node1 acc.	Node2 acc.	Node1 annotation	Node2 annotation	Score
AT2G29500	cpHsc70-1	AT2G29500.1	AT4G24280.1	HSP20 family protein	chloroplast heat shock protein 70-1; acts redundantly with HSP70-7 in the thermotolerance of germinating seeds; plays an important role in the protein precursor import into chloroplasts	0.665
AT5G16450	TPI	AT5G16450.1	AT3G55440.1	regulator of ribonuclease-like protein 2; catalyzes the aldol cleavage of 4-hydroxy-4-methyl-2- oxoglutarate (HMG) into 2 molecules of pyruvate; also contains a secondary oxaloacetate (OAA) decarboxylase activity due to the common pyruvate enolate transition state formed following C-C bond cleavage in the retro-aldol and decarboxylation reactions (by similarity)	triosephosphate isomerase	0.533
CPN60A	EMB3113	AT2G28000.1	AT2G33800.1	chaperonin-60α; binds Rubisco small and large subunits and is implicated in the assembly of the enzyme oligomer; involved in protein assisted folding; required for proper chloroplast development	embryo defective 3113; binds directly to 16S ribosomal RNA	0.567
CPN60A	SAM1	AT2G28000.1	AT1G02500.1	chaperonin-60α; binds Rubisco small and large subunits and is implicated in the assembly of the enzyme oligomer; involved in protein assisted folding; required for proper chloroplast development	S-adenosylmethionine synthetase 1; catalyzes the formation of S-adenosylmethionine from methionine and ATP; the overall synthetic reaction is composed of two sequential steps, AdoMet formation and the subsequent tripolyphosphate hydrolysis which occurs prior to release of AdoMet from the enzyme	0.642
CPN60A	TPI	AT2G28000.1	AT3G55440.1	chaperonin-60α; binds Rubisco small and large subunits and is implicated in the assembly of the enzyme oligomer; involved in protein assisted folding, required for proper chloroplast development	triosephosphate isomerase	0.479
CPN60A	cpHsc70-1	AT2G28000.1	AT4G24280.1	chaperonin-6α; binds Rubisco small and large subunits and is implicated in the assembly of the enzyme oligomer; involved in protein assisted folding; required for proper chloroplast development	Chloroplast heat shock protein 70-1; acts redundantly with HSP70-7 in the thermotolerance of germinating seeds; plays an important role in the protein precursor import into chloroplasts	0.995

Node1	Node2	Node1 acc.	Node2 acc.	Node1 annotation	Node2 annotation	Score
CPN60A	mMDH1	AT2G28000.1	AT1G53240.1	chaperonin-60α; binds Rubisco small and large subunits and is implicated in the assembly of the enzyme oligomer; involved in protein assisted folding; required for proper chloroplast development	malate dehydrogenase 1	0.76
EMB3113	CPN60A	AT2G33800.1	AT2G28000.1	embryo defective 3113; binds directly to 16S ribosomal RNA	chaperonin-60α; binds Rubisco small and large subunits and is implicated in the assembly of the enzyme oligomer; involved in protein assisted folding; required for proper chloroplast development	0.567
EMB3113	cpHsc70-1	AT2G33800.1	AT4G24280.1	embryo defective 3113; binds directly to 16S ribosomal RNA	chloroplast heat shock protein 70-1; acts redundantly with HSP70-7 in the thermotolerance of germinating seeds; plays an important role in the protein precursor import into chloroplasts	0.495
FBA1	FNR1	AT2G21330.1	AT5G66190.1	fructose-bisphosphate aldolase 1	ferredoxin--NADP+ reductase; plays a key role in regulating the relative amounts of cyclic and non-cyclic electron flow to meet the demands of the plant for ATP and reducing power	0.631
FBA1	TPI	AT2G21330.1	AT3G55440.1	fructose-bisphosphate aldolase 1	triosephosphate isomerase	0.842
FNR1	FBA1	AT5G66190.1	AT2G21330.1	ferredoxin--NADP+ reductase; plays a key role in regulating the relative amounts of cyclic and non-cyclic electron flow to meet the demands of the plant for ATP and reducing power	fructose-bisphosphate aldolase 1	0.631
SAM1	CPN60A	AT1G02500.1	AT2G28000.1	S-adenosylmethionine synthetase 1; catalyzes the formation of S-adenosylmethionine from methionine and ATP; the overall synthetic reaction is composed of two sequential steps, AdoMet formation and the subsequent tripolyphosphate hydrolysis which occurs prior to release of AdoMet from the enzyme	chaperonin-60α; binds Rubisco small and large subunits and is implicated in the assembly of the enzyme oligomer; involved in protein assisted folding; required for proper chloroplast development	0.642
SAM1	TPI	AT1G02500.1	AT3G55440.1	S-adenosylmethionine synthetase 1; catalyzes the formation of S-adenosylmethionine from methionine and ATP. The overall synthetic reaction is composed of two sequential steps, AdoMet formation and the subsequent tripolyphosphate hydrolysis which occurs prior to release of AdoMet from the enzyme	triosephosphate isomerase	0.405

Node1	Node2	Node1 acc.	Node2 acc.	Node1 annotation	Node2 annotation	Score
TPI	AT5G16450	AT3G55440.1	AT5G16450.1	triosephosphate isomerase	regulator of ribonuclease-like protein 2; catalyzes the aldol cleavage of 4-hydroxy-4-methyl-2- oxoglutarate (HMG) into 2 molecules of pyruvate; also contains a secondary oxaloacetate (OAA) decarboxylase activity due to the common pyruvate enolate transition state formed following C-C bond cleavage in the retro-aldol and decarboxylation reactions (by similarity)	0.533
TPI	CPN60A	AT3G55440.1	AT2G28000.1	triosephosphate isomerase	chaperonin-60α; binds Rubisco small and large subunits and is implicated in the assembly of the enzyme oligome; involved in protein assisted folding; required for proper chloroplast development	0.479
TPI	FBA1	AT3G55440.1	AT2G21330.1	triosephosphate isomerase	fructose-bisphosphate aldolase 1	0.842
TPI	SAM1	AT3G55440.1	AT1G02500.1	triosephosphate isomerase	S-adenosylmethionine synthetase 1; catalyzes the formation of S-adenosyl-methionine from methionine and ATP. The overall synthetic reaction is composed of two sequential steps, AdoMet formation and the subsequent tripolyphosphate hydrolysis which occurs prior to release of AdoMet from the enzyme	0.405
TPI	cpHsc70-1	AT3G55440.1	AT4G24280.1	triosephosphate isomerase	chloroplast heat shock protein 70-1;aActs redundantly with HSP70-7 in the thermo-tolerance of germinating seed; plays an important role in the protein precursor import into chloroplasts	0.41
TPI	mMDH1	AT3G55440.1	AT1G53240.1	triosephosphate isomerase	malate dehydrogenase 1	0.674
cpHsc70-1	AT2G29500	AT4G24280.1	AT2G29500.1	chloroplast heat shock protein 70-1; acts redundantly with HSP70-7 in the thermotolerance of germinating seeds; plays an important role in the protein precursor import into chloroplasts	HSP20 family protein	0.665
cpHsc70-1	CPN60A	AT4G24280.1	AT2G28000.1	chloroplast heat shock protein 70-1; acts redundantly with HSP70-7 in the thermotolerance of germinating seed; plays an important role in the protein precursor import into chloroplasts	chaperonin-60α; binds Rubisco small and large subunits and is implicated in the assembly of the enzyme oligomer; involved in protein assisted folding; required for proper chloroplast development	0.995
cpHsc70-1	EMB3113	AT4G24280.1	AT2G33800.1	chloroplast heat shock protein 70-1; acts redundantly with HSP70-7 in the thermotolerance of germinating seed; plays an important role in the protein precursor import into chloroplasts	embryo defective 3113; binds directly to 16S ribosomal RNA	0.495

Node1	Node2	Node1 acc.	Node2 acc.	Node1 annotation	Node2 annotation	Score
cpHsc70-1	TPI	AT4G24280.1	AT3G55440.1	chloroplast heat shock protein 70-1; acts redundantly with HSP70-7 in the thermotolerance of germinating seeds; plays an important role in the protein precursor import into chloroplasts	triosephosphate isomerase	0.41
cpHsc70-1	mMDH1	AT4G24280.1	AT1G53240.1	chloroplast heat shock protein 70-1; acts redundantly with HSP70-7 in the thermotolerance of germinating seeds; plays an important role in the protein precursor import into chloroplasts	malate dehydrogenase 1	0.405
mMDH1	CPN60A	AT1G53240.1	AT2G28000.1	malate dehydrogenase 1	chaperonin-60α; binds Rubisco small and large subunits and is implicated in the assembly of the enzyme oligomer; involved in protein assisted folding; required for proper chloroplast development	0.76
mMDH1	TPI	AT1G53240.1	AT3G55440.1	malate dehydrogenase 1	triosephosphate isomerase	0.674
mMDH1	cpHsc70-1	AT1G53240.1	AT4G24280.1	malate dehydrogenase 1	chloroplast heat shock protein 70-1; Acts redundantly with HSP70-7 in the thermotolerance of germinating seeds; plays an important role in the protein precursor import into chloroplasts	0.405

Table 4 Suppl. The abbreviations of protein names showed in the networks of Fig. 5.

SAM1	S-adenosylmethionine synthetase 1; catalyzes the formation of S-adenosylmethionine from methionine and ATP; the overall synthetic reaction is composed of two sequential steps, AdoMet formation and the subsequent tripolyphosphate hydrolysis which occurs prior to release of AdoMet from the enzyme (393 aa)
mMDH1	malate dehydrogenase 1 (341 aa)
FBA1	fructose-bisphosphate aldolase 1 (399 aa)
CPN60A	chaperonin-60α; binds Rubisco small and large subunits and is implicated in the assembly of the enzyme oligomer; involved in protein assisted folding; required for proper chloroplast development (586 aa)
AT2G29500	HSP20 family protein (153 aa)
EMB3113	embryo defective 3113; binds directly to 16S ribosomal RNA (303 aa)
PDX1.1	pyridoxine biosynthesis 1.1; catalyzes the formation of pyridoxal 5'-phosphate from ribose 5-phosphate (RBP), glyceraldehyde 3-phosphate (G3P) and ammonia; the ammonia is provided by PDX2; can also use ribulose 5- phosphate and dihydroxyacetone phosphate as substrates, resulting from enzyme-catalyzed isomerization of RBP and G3P, respectively; also plays an indirect role in resistance to singlet oxygen- generating photosensitizers (309 aa)
TPI	triosephosphate isomerase (254 aa)
cpHsc70-1	chloroplast heat shock protein 70-1; acts redundantly with HSP70-7 in the thermotolerance of germinating seeds; plays an important role in the protein precursor import into chloroplasts (718 aa)
AT5G16450	regulator of ribonuclease-like protein 2; catalyzes the aldol cleavage of 4-hydroxy-4-methyl-2- oxoglutarate (HMG) into 2 molecules of pyruvate; also contains a secondary oxaloacetate (OAA) decarboxylase activity due to the common pyruvate enolate transition state formed following C-C bond cleavage in the retro-aldol and decarboxylation reactions (By similarity) (166 aa)
PBB2	20S proteasome β subunit PBB2; the proteasome is a multicatalytic proteinase complex which is characterized by its ability to cleave peptides with Arg, Phe, Tyr, Leu, and Glu adjacent to the leaving group at neutral or slightly basic pH; the proteasome has an ATP-dependent proteolytic activity (274 aa)
FNR1	ferredoxin--NADP+ reductase; plays a key role in regulating the relative amounts of cyclic and non-cyclic electron flow to meet the demands of the plant for ATP and reducing power (360 aa)

Table 5 Suppl. A list of identified proteins (detailed information) in the 10-leaf and the flowering stages under waterlogging stress (SN - spot number on the master gel, AN - accession number of the identified proteins regarding the NCBI database, PS - score of the identified peptides, PM - number of matched peptide, the proteins with more than three matched peptides were considered, PC - protein coverage of the identified proteins, FDR - false discovery rate.

SN	AN	Protein description	PS	Exp. Mr/pI	Theor. Mr/pI	PM	PC	Peptide sequence	FDR values
Ten-leaf stage									
112	HSP7S_SPIOL	stromal 70 kDa heat shock-related protein	1750	64918/4.87	64900.46/4.87	70	19.2	IAGLEVLR	0.05
144	RUBA_RICCO	Rubisco large subunit-binding protein subunit α (fragment)	1540	51461/4.77	52378.84/4.77	54	31.7	LGADILQK	0.05
328	ALFC_SPIOL	fructose-bisphosphate aldolase	248	42727/6.85	42468.30/6.85	20	13.5	EAAWGLAR	0.05
344	PGKY_WHEAT	phosphoglycerate kinase	38	42153/8.7	42121.96/5.64	10	8.7	IGVIESLLEK	0.05
433	TPIS_ARATH	triosephosphate isomerase	61	27380/5.39	27169.08/5.39	4	7.1	FFVGGNWK	0.05
357	CYSK_CITLA	cysteine synthase	93	34492/6.25	34342.71/6.26	3	10.8	EGLLVGISSGAAAAAAIR	0.05
363	PSBO_HELAN	oxygen-evolving enhancer protein 1	234	34487/5.4	34223.66/5.40	7	15.1	FCLEPTSFTVK	0.05
369	PSBO_SOLLC	oxygen-evolving enhancer protein 1	3876	35154/5.91	34947.57/5.89	138	23.1	GSSFLDPK	0.05
600	UCRIA_SOLTU	cytochrome *b6-f* complex iron-sulfur subunit	351	24593/8.2	24266.81/8.20	27	10.0	CMAASIPADDR	0.05
375	PDX11_ARATH	pyridoxal biosynthesis protein PDX1.1	44	33126/5.75	32861.92/5.73	2	7.4	VGLAQMLR	0.05
529	CB11_SOLLC	chlorophyll *a-b* binding protein 6A	532	26786/5.82	26574.67/5.83	17	14.6	YPGGAFDPLGYSK	0.05
542	CB22_HORVU	chlorophyll *a-b* binding protein 2	100	28147/5.69	28050.97/5.69	4	9.5	FGEAVWFK	0.05
570	YPTC5_CHLRE	GTP-binding protein YPTC5	27	23470/5.73	23142.25/5.73	3	16.5	VIILGDSGVGK	0.05
646	TRXM_MAIZE	thioredoxin M-type	30	18460/8.7	18073.10/8.69	2	5.4	SIPTVLIFK	0.05
656	RBS_MANES	Rubisco small chain	1088	20625/8.65	20410.63/8.66	75	22.0	YWTMWK	0.05
668	RBS1_SOYBN	Rubisco small chain 1	150	20288/8.87	20073.36/8.87	47	25.8	SPGYYDGR	0.05
200	RCA_ORYSJ	Rubisco activase	259	51764/5.43	51454.29/5.43	13	16.1	VYDDEVR	0.05
234	RCA2_LARTR	Rubisco activase 2	993	48251/6.78	48053.85/6.78	23	23.7	SFQCELVFAK	0.05
272	ALFC1_ARATH	probable fructose-bisphosphate aldolase 1	162	43075/6.18	42930.94/6.18	10	20.6	EAAWGLAR	0.05
579	SODCP_SPIOL	superoxide dismutase [Cu-Zn]	3826	22667/5.88	22567.17/5.88	110	10.8	GTSNVEGVVTLTQEDDGPTTVNVR	0.05
Flowering stage									
59	HSP7F_ARATH	heat shock 70 kDa protein 6	886	76575/5.07	76508.02/5.07	41	22.7	GVPQIEVK	0.05
143	FNRL1_ARATH	ferredoxin--NADP reductase, leaf isozyme 1	550	40643/8.32	40326.46/8.32	18	11.1	DGIDWLEYKK	0.05
154	METK1_ARATH	S-adenosylmethionine synthase 1	688	43587/5.51	43158.05/5.51	30	33.8	TIFHLNPSGR	0.05
199	MDHM1_ARATH	malate dehydrogenase 1	233	36010/8.54	35804.46/8.54	7	6.7	EGLEALKPELK	0.05
424	HS17B_ARATH	17.6 kDa class I heat shock protein 2	23	17552/6.33	17562.82/6.33	4	15.0	LPENVKMDQVK	0.05
86	CPNA1_ARATH	chaperonin 60 subunit α 1	44	62205/5.09	62072.01/5.08	5	6.5	DIIPILEK	0.05
106	ATPB_PHAAO	ATP synthase subunit β	584	53998/5.44	53974.90/5.44	37	30.9	IGLFGGAGVGK	0.05
180	ATPB_BLEOC	ATP synthase subunit β	523	42392/4.94	42417.93/4.94	17	14.9	IGLFGGAGVGK	0.05
163	PGKY_TOBAC	phosphoglycerate kinase	443	42338/5.69	42364.07/5.69	28	13.5	GVTPKYSLKPLVPR	0.05
173	KPPR_SPIOL	phosphoribulokinase	414	45321/5.82	45007.16/5.82	15	21.4	LTCSYPGIK	0.05
183	G3PA_PEA	glyceraldehyde-3-phosphate dehydrogenase A	2229	43597/8.8	43338.43/8.80	61	17.0	VVDLADIVANNWK	0.05
187	G3PC_ANTMA	glyceraldehyde-3-phosphate dehydrogenase	2009	36776/8.3	36685.03/8.30	81	33.2	VLPQLNGK	0.05
201	G3PC_DIACA	glyceraldehyde-3-phosphate dehydrogenase	236	37105/6.46	36900.19/6.46	18	23.4	TLLFGEK	0.05
207	F16P2_SOLTU	fructose-1,6-bisphosphatase	238	37743/5.8	37310.62/5.80	9	7.9	LDVLSNEVFIK	0.05
176	GLNA1_MEDSA	glutamine synthetase cytosolic isozyme	3538	39254/5.49	39107.13/5.49	139	18.5	IIAEYIWIGGSGLDLR	0.05
248	CYSK2_BRAJU	cysteine synthase	17	34225/5.51	34132.45/5.51	3	10.8	IDGFISGIGTGGTITGAGK	0.05
210	CAS1_MALDO	L-3-cyanoalanine synthase 1	181	41085/7.6	40883.21/7.61	17	13.6	VTEGCGAYIAVK	0.05
235	PSBO_SOLLC	oxygen-evolving enhancer protein 1	41	35154/5.91	34947.57/5.89	5	11.2	DGIDYAAVTVQLPGGER	0.05
237	PSBO_HELAN	oxygen-evolving enhancer protein 1	137	34487/5.4	34223.66/5.40	4	13.6	RLTYDEIQSK	0.05
236	RR5_ARATH	30S ribosomal protein S5	368	32682/8.99	32645.13/8.99	14	21.1	GIPMEELWK	0.05
419	RRAA2_ARATH	putative 4-hydroxy-4-methyl-2-oxoglutarate aldolase 2	50	18094/5.42	17820.36/5.42	2	6.6	ALQPIFQIYGR	0.05
287	CB4B_SOLLC	chlorophyll a-b binding protein CP24 10B	71	27453/6.31	27470.53/6.31	3	7.4	LKLAEIK	0.05
295	KAD4_ORYSJ	adenylate kinase 4	78	26886/7.64	26674.95/7.65	6	20.2	GFILDGFPR	0.05

SN	AN	Protein description	PS	Exp. Mr/pI	Theor. Mr/pI	PM	PC	Peptide sequence	FDR values
333	PSB7B_ARATH	proteasome subunit beta type-7-B	81	29940/6.71	29617.00/6.71	4	6.2	VVTALTLLK	0.05
354	PSB1_ORYSJ	proteasome subunit beta type-1	109	24608/6.43	24281.58/6.42	4	7.2	DAVTPLSETEAVDLVK	0.05
338	NDHK_CHAVU	NAD(P)H-quinone oxidoreductase subunit K	22	27985/7.62	27660.74/7.61	4	22.1	QADLIITAGTVTMK	0.05
418	RBS1_PETHY	Rubisco small chain SSU8	35	20585/8.29	20370.36/8.28	5	24.4	YWTMWK	0.05
347	RANA1_TOBAC	GTP-binding nuclear protein Ran-A1	33	25345/6.38	25018.48/6.38	4	25.8	NLQYYEISAK	0.05
350	RAN2_ORYSI	GTP-binding nuclear protein Ran-2	43	25365/6.66	25038.65/6.65	3	19.0	LVIVGDGGTGK	0.05

Table 6 Suppl. Spot densitometric and fold change analyses in the 10-leaf stage under waterlogging stress; 2 d, 3 d - waterlogging for 2 days or 3 days.

Spot No.	Average normalized volumes			Fold change		Fold change		
	control	2 d	3 d	2 d	3 d	control	2 d	3 d
112	2686000	2717000	5315000	1.011541	1.978779	1	1.011541	1.978779
144	10740000	7069000	8668000	0.658194	0.807076	1	-1.51931	-1.23904
200	11730000	5846000	10320000	0.498380	0.879795	1	-2.00650	-1.13663
234	30810000	21880000	25160000	0.710159	0.816618	1	-1.40814	-1.22456
272	11650000	8528000	7938000	0.732017	0.681373	1	-1.36609	-1.46762
328	2572000	4194000	2631000	1.630638	1.022939	1	1.630638	1.022939
344	10220000	5992000	7114000	0.586301	0.696086	1	-1.70561	-1.43660
357	5024000	7448000	6972000	1.482484	1.387739	1	1.482484	1.387739
363	2667000	4449000	5003000	1.668166	1.875891	1	1.668166	1.875891
369	23710000	36840000	38120000	1.553775	1.60776	1	1.553775	1.607760
375	753500	1253000	1728000	1.662906	2.293298	1	1.662906	2.293298
433	54880000	33240000	43260000	0.605685	0.788265	1	-1.65102	-1.26861
529	817800	529200	446300	0.647102	0.545732	1	-1.54535	-1.83240
542	1417000	1387000	2420000	0.978829	1.707833	1	-1.02163	1.707833
570	2303000	902000	1193000	0.391663	0.518020	1	-2.55322	-1.93043
579	2237000	6282000	7118000	2.808225	3.181940	1	2.808225	3.181940
600	24830000	18090000	16780000	0.728554	0.675795	1	-1.37258	-1.47974
646	2098000	7506000	3648000	3.577693	1.738799	1	3.577693	1.738799
656	33440000	25070000	22010000	0.749701	0.658194	1	-1.33387	-1.51931
668	15800000	11110000	8880000	0.703165	0.562025	1	-1.42214	-1.77928

Table 7 Suppl. Spot densitometric and fold change analyses in the flowering stage under waterlogging stress; 2 d, 3 d - waterlogging for 2 days or 3 days.

Spot No.	Fold	Average normalized volumes			Fold change		Fold change		
		control	2 d	3 d	2 d	3 d	control	2 d	3 d
59	5.2	3561000	5311000	18520000	1.491435	5.200786	1	1.491435	5.200786
86	4.1	2715000	11080000	4830000	4.081031	1.779006	1	4.081031	1.779006
106	1.6	3747000	5912000	4673000	1.577796	1.247131	1	1.577796	1.247131
143	1.6	2085000	1294000	1346000	0.620624	0.645564	1	-1.61128	-1.54903
150	2.3	34290000	79130000	34790000	2.307670	1.014582	1	2.307670	1.014582
154	2.1	1689000	1534000	3252000	0.90823	1.925400	1	-1.10104	1.925400
163	1.5	3078000	2295000	3504000	0.745614	1.138402	1	-1.34118	1.138402
173	1.6	13500000	9876000	8208000	0.731556	0.60800	1	-1.36695	-1.64474
176	1.7	79340000	45770000	47710000	0.576884	0.601336	1	-1.73345	-1.66296
180	1.8	18210000	32860000	27160000	1.804503	1.491488	1	1.804503	1.491488
183	1.7	9322000	10790000	16070000	1.157477	1.723879	1	1.157477	1.723879
187	1.6	2480000	3471000	3942000	1.399597	1.589516	1	1.399597	1.589516
199	1.8	11150000	15410000	20220000	1.382063	1.813453	1	1.382063	1.813453
201	1.8	19360000	11270000	10730000	0.582128	0.554236	1	-1.71783	-1.80429
207	1.7	2706000	4546000	3143000	1.679970	1.161493	1	1.679970	1.161493
210	3.1	6138000	2343000	2007000	0.381720	0.326979	1	-2.61972	-3.05830
235	1.6	3995000	5873000	6555000	1.470088	1.640801	1	1.470088	1.640801
236	2.7	16150000	5883000	6719000	0.364272	0.416037	1	-2.74520	-2.40363
237	1.5	987400	700700	1062000	0.709641	1.075552	1	-1.40916	1.075552
248	1.7	3257000	1965000	2894000	0.603316	0.888548	1	-1.65751	-1.12543
287	1.5	7602000	9273000	6083000	1.219811	0.800184	1	1.219811	0.800184
295	1.6	4147000	2969000	4613000	0.715939	1.112370	1	-1.39677	1.112370
333	1.4	5411000	7827000	5422000	1.446498	1.002033	1	1.446498	1.002033
338	1.4	14370000	20460000	20780000	1.423800	1.446068	1	1.423800	1.446068
347	2	4152000	6143000	8403000	1.479528	2.023844	1	1.479528	2.023844
350	1.4	10860000	9028000	7708000	0.831308	0.709761	1	-1.20292	-1.40893
354	2.8	8363000	23560000	16530000	2.817171	1.976563	1	2.817171	1.976563
401	2.4	3256000	1665000	1377000	0.511364	0.422912	1	-1.95556	-2.36456
418	1.9	6090000	6059000	3181000	0.994910	0.522332	1	-1.00512	-1.91449
419	2.3	7740000	4634000	3335000	0.598708	0.430879	1	-1.67026	-2.32084
424	2.1	4806000	9442000	9960000	1.964628	2.072409	1	1.964628	2.072409

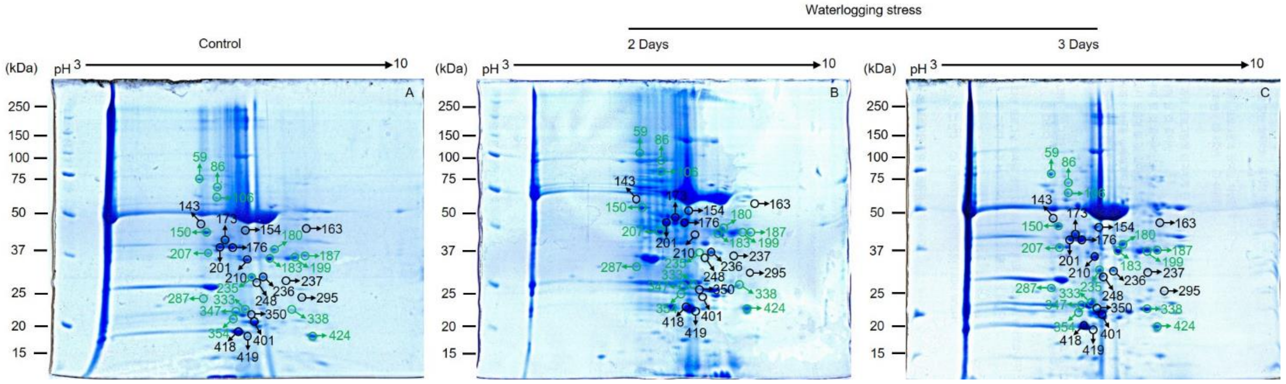

Fig. 1 Suppl. Representative two-dimensional electrophoresis maps of the identified proteins in the sesame at the flowering stage: *A* - control; *B* - waterlogging for 2 d; *C* - waterlogging for 3 d.

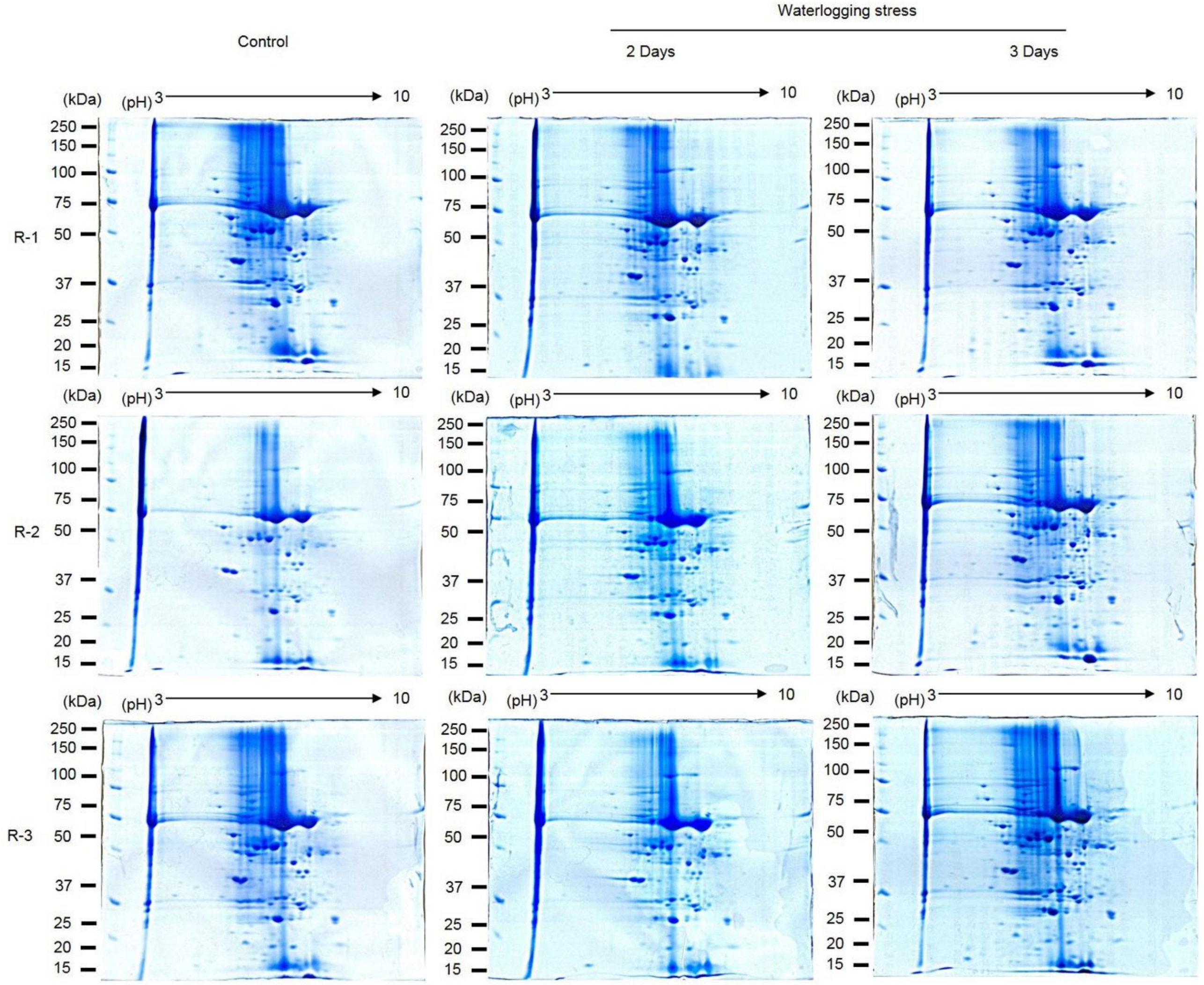

Fig. 2 Suppl. A two-dimensional electrophoresis pattern of proteins in the leaves of sesame grown under control and waterlogging conditions imposed at the 10-leaf stage. R-1, R-2, and R-3 denote replications.

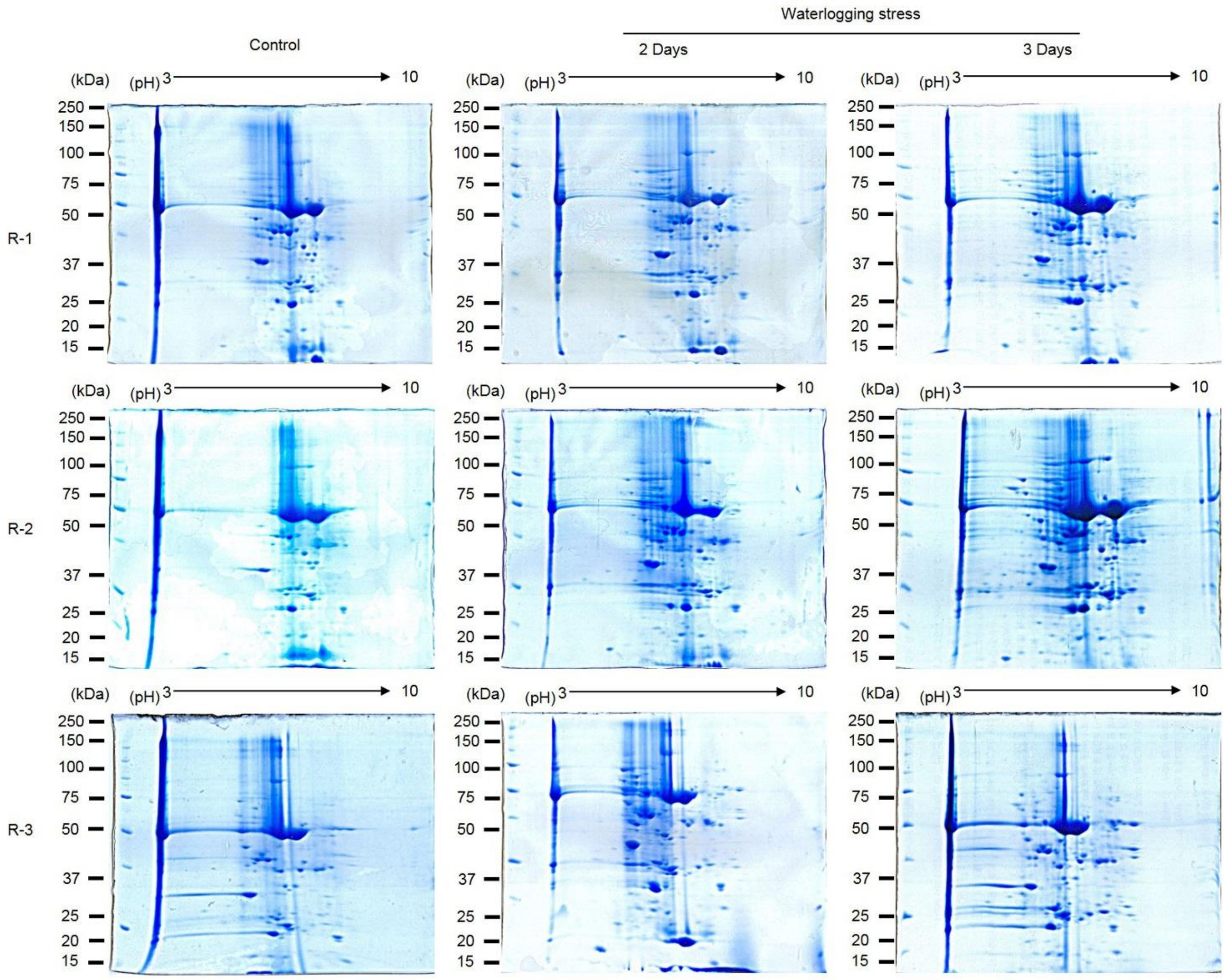

Fig. 3 Suppl. A two-dimensional electrophoresis pattern of proteins in the leaves of sesame grown under control and waterlogging conditions imposed at the flowering stage. R-1, R-2, and R-3 denote replications.

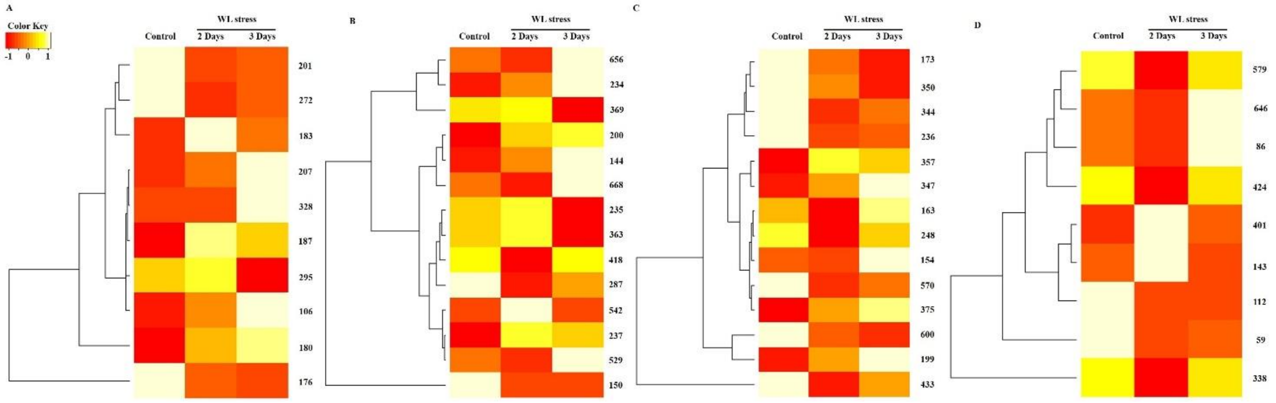

Fig. 4 Suppl. Hierarchical clustering differentially abundant proteins with similar functions under waterlogging stress. *A* - Proteins related to photosynthesis; *B* - proteins related to stress and defense; *C* - proteins related to energy and saccharide metabolism; *D* - proteins related to protein biosynthesis and metabolism.

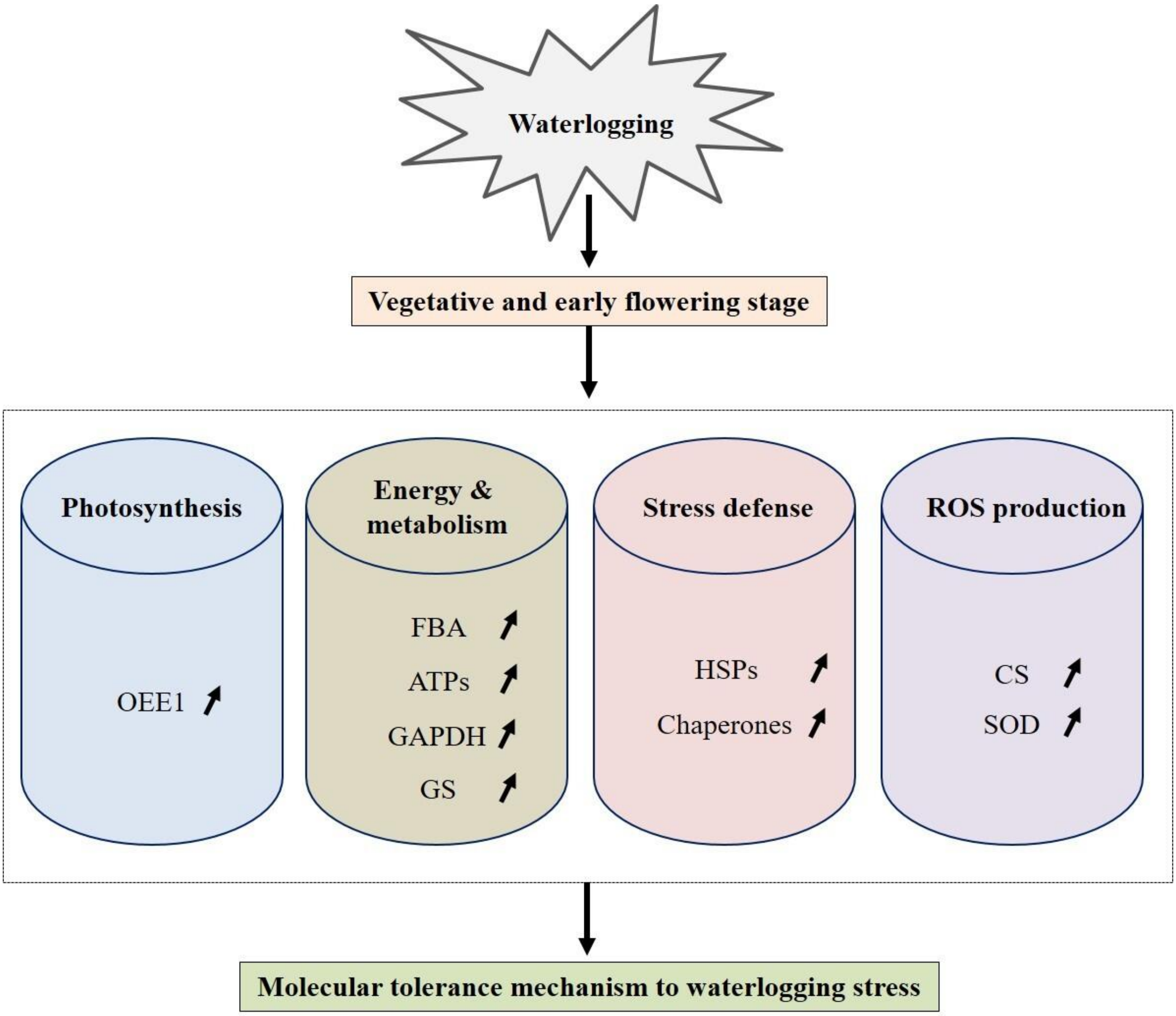

Fig. 5 Suppl. A hypothetically integrated schematic diagram of the mechanism involved in waterlogging tolerance in sesame. An *arrow* (↗) indicates increased abundance. OEE1 - oxygen-evolving enhancer protein; FBA - fructose-1,6-*bis*phosphate aldolase; ATPS - ATP synthase; GAPDH - glyceraldehyde-3-phosphate dehydrogenase; GS - glutamine synthetase; HSPs - heat shock proteins; CS - cysteine synthase; SOD - superoxide dismutase.